

# Dust formation in carbon-rich Wolf-Rayet stars<sup>\*</sup>

## I. Chemistry of small carbon clusters and silicon species

I. Cherchneff<sup>1</sup>, Y.H. Le Teuff<sup>1</sup>, P.M. Williams<sup>2</sup>, and A.G.G.M. Tielens<sup>3</sup>

<sup>1</sup> Department of Physics, UMIST, P.O. Box 88, Manchester M60 1QD, UK

<sup>2</sup> Royal Observatory, Blackford Hill, Edinburgh EH9 3HJ, UK

<sup>3</sup> Kapteyn Institute, University of Groningen, P.O. Box 800, 9700 Groningen, The Netherlands

Received 23 April 1998 / Accepted 25 August 1999

**Abstract.** The formation of small carbon chains and molecular precursors to silicon carbide grains is investigated in the hot, hostile environment of carbon-rich Wolf-Rayet (WC) winds. We consider only WC stars which produce dust on a continuous basis and develop for the first time non-equilibrium, chemical kinetic routes to nucleating dust precursors in the outflow. These can be used to calculate quantitatively the yield of such dust precursors for various outflow scenarios. Because WC stars have lost all their hydrogen in the WN phase, the chemical processes used in the model involve a pure helium, carbon, oxygen, silicon and sulphur chemistry which resembles that encountered in graphite or metal vaporization experiments in the laboratory. We derive abundances for small linear carbon clusters up to C<sub>6</sub> and silicon-bearing species for various wind parameters and conclude that high-density regions in the form of clumps or discs are of paramount importance to the formation of dust in WC stars.

**Key words:** molecular data – molecular processes – stars: circumstellar matter – stars: Wolf-Rayet

### 1. Introduction

Wolf-Rayet (WR) stars represent a late stage in the evolution of massive stars before the supernova explosion episode. WR stars are characterised by high effective temperatures ( $T_{\star} \sim 20000 - 90000\text{K}$ ), fast radiatively accelerated winds ( $V_{wind} \sim 1000 - 4000 \text{ km s}^{-1}$ ), high mass loss rates ( $\dot{M} \sim 10^{-5} M_{\odot} \text{ yr}^{-1}$ ) which expel almost half of the initial ZAMS stellar masses to the surrounding medium (van der Hucht 1998). The winds of these objects are also the site of strong emission lines arising from excited atoms and ions and continuum free-free emission at infrared (IR) and radio wavelengths. WR stars experience three phases of evolution corresponding to different emission spectra: the WN phase is characterised by hydrogen burning in the core

via the CNO cycle, and enhancement of helium and nitrogen as a result. The hydrogen abundance reflects the completeness of this process. The more evolved WC phase corresponds to helium burning in the core via the triple-alpha process accompanied by weak s-processes. WC stars are rich in helium and carbon, have varying amounts of oxygen and are deficient in hydrogen and nitrogen. Those with the most oxygen, whose spectra show conspicuous O VI emission lines, are classified WO stars. Therefore, the elemental composition at the stellar surface resulting from the various nuclear burning stages governs the wind chemistry and the type of dust formed in the outflow. As WC stars have no hydrogen left in their atmosphere, the wind elemental composition is dominated by helium, carbon and oxygen, mainly in their ionic forms due to the strong stellar radiation field.

Dust was first observed in WC stars of spectral type WC9 by Allen et al. (1972). Later photometric studies in the infrared by Williams et al. (1987, hereafter WHT) have shown that half of the WC8 and most of the WC9 stars were condensing dust in their wind steadily or episodically. The objects for which the dust was always observed had to be forming fresh grains on a continuous basis because dust particles were momentum-coupled to the fast stellar wind and thus being continuously carried away from the stars. WHT modelled the IR spectral energy distributions of the dust-making WC stars, finding that these could be well fitted with shells of amorphous carbon (AC) grains in radiative equilibrium with the stellar radiation field. Other condensates have also been considered with less success in reproducing the near-IR stellar spectra (Dyck et al. 1984). New observations with the Short Wavelength Spectrometer (SWS) on board the ISO satellite were conducted for various WC stars by van der Hucht et al. (1996) and full spectral energy distributions in the IR were obtained for these objects. Again, models by Williams et al. (1997) can reproduce well the ISO data using homogeneous shells of AC dust grains.

In addition to the IR emission, dust formation in WC stars has manifested itself by eclipse-like variations recently attributed to episodic obscuration of starlight by blobs of dust in the line-of-sight very close to the star (Veen et al. 1998). These variations appear to be similar to those of the R Corinae Borealis (R CrB) stars but with smaller amplitudes and the

Send offprint requests to: Y.H. Le Teuff

<sup>\*</sup> Appendix A is only available in electronic form at the CDS via anonymous ftp to cdsarc.u-strasbg.fr (130.79.128.5) or via <http://cdsweb.u-strasbg.fr/Abstract.html>

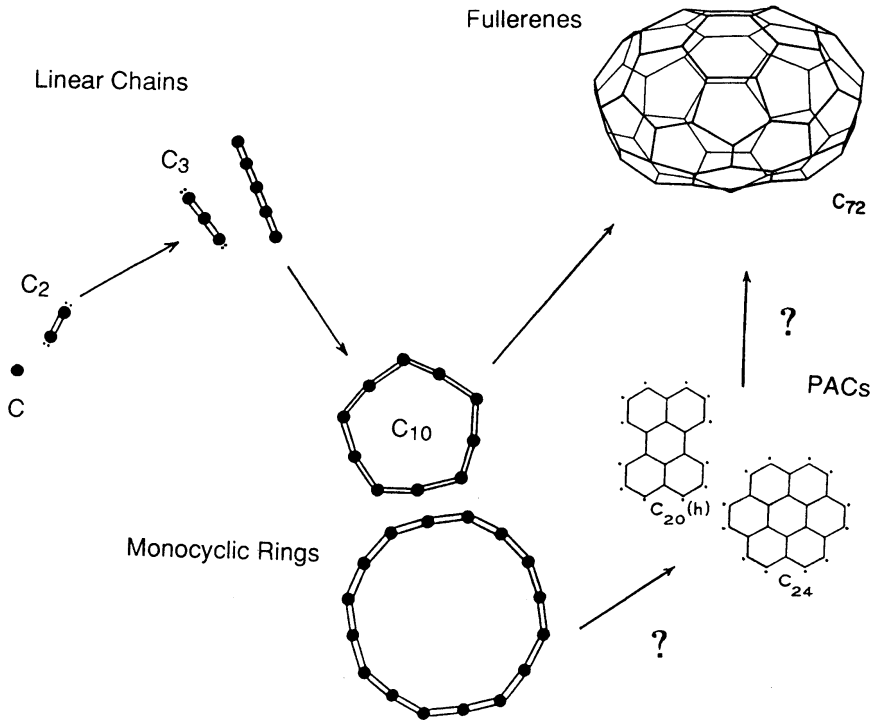


**Fig. 1.** The dominant structural pathways to the formation of AC grains in a hydrogen-poor gas adapted from Cherchneff & Tielens (1995). The route to fullerene via PAC molecules is now questionable in view of new experimental results (see text).

mechanism triggering blob formation is still unknown. Comparison of the spectra of the archetypical dust-forming WC9 star WR104 (Ve2-45) during such an episode and under normal conditions showed that the dust was forming rather close to the star (Crowther 1997) and within the inner dust shells derived by WHT and Williams et al. (1997).

Silicon carbide clusters are responsible for the emission/absorption band at  $11.3 \mu\text{m}$  in carbon-rich AGB stars. Such a feature is not detected in WC stars although silicon is present in the stellar wind as proved by the detection of ionic silicon forbidden IR lines in emission in the line forming region (Williams et al. 1997). The absence of SiC signature is puzzling and may hint at the fact that the chemical processes responsible for the formation of SiC in late-type stars may be hindered in the hydrogen-deficient WC wind.

In this paper, we extend the previous study of Cherchneff & Tielens (1995) and describe the first steps of dust nucleation in hydrogen-deficient environments using a chemical kinetic approach. Such a study has a more general relevance and could be applied as well to the He-burning zones of supernova ejecta and to R CrB stars. We do not attempt to construct a wind model for a WC star but we prefer testing the chemistry describing the formation of small carbon clusters and silicon-bearing species for the physical conditions encountered at the inner radius of the dust shells used in the models of WHT and Williams et al. (1997). In Sect. 2, we discuss the nature of carbon dust condensing in a hydrogen-poor environment and the potential precursors to the nucleation of silicon carbides. The chemical and stellar models are described in Sect. 3. Finally, results are presented in Sect. 4 and we discuss the possible wind geometries leading to dust nucleation and condensation and related issues in Sect. 5.

## 2. The nature of dust and its precursors

Amorphous carbon grains can easily be formed in the laboratory in a hydrogen-free environment from vaporisation of graphite rods. This type of experiment has led to the discovery of fullerenes by Kroto et al. (1985). Graphite vaporisation usually occurs at temperatures of a few thousand degrees Kelvin but at high gas density as a buffer gas (usually helium) is used to carry the gaseous products out of the hot vaporisation zone. The resulting products represent various families of carbon clusters, from linear chains to rings and fullerene molecules.

Since the discovery of C<sub>60</sub>, many studies have focused on carbon clusters and our understanding of fullerene and AC grains synthesis has been revised with time. Because of the lack of hydrogen in the gas, the formation of pure carbon clusters will proceed from the nucleation of very small clusters, as illustrated in Fig. 1. The most stable structure is linear up to 10 carbon atoms (Heath 1992) resulting in small carbon chains with unsatisfied bonds at each end, but ring isomers can also co-exist along with the linear chains for clusters with 8, 9 and 10 carbon atoms (von Helden et al. 1994). The ring structure becomes more stable for species with  $N(C) > 10$  and monocyclic rings form and coalesce into bicyclic and possibly tricyclic rings (von Helden et al. 1993; Shemilov et al. 1994). However, Shemilov et al. shows that a bicyclic ring can isomer quickly to a large monocyclic ring for clusters with  $24 < N(C) < 36$  during annealing, and that graphitic fragments ( $\equiv$  large polycyclic aromatic carbons, or PACs) exist but in small quantities compared to monocyclic rings.

These results have changed our view on how fullerene is formed from small carbon clusters. It was initially thought that fullerene grew from the curling of aromatic sheets due to the

**Table 1.** Stellar and wind parameters for the standard WC9 star used in our model.

Star	Dust Inner Shell
$T_{eff} = 19000 \text{ K}$	$R_{inner} = 760 R_{\star}$
$R_{\star} = 12 R_{\odot}$	$T_{gas} = 4000 \text{ K}$
$\dot{M} = 10^{-5} M_{\odot} \text{ yr}^{-1}$	$n_{gas} = 10^6 \text{ cm}^{-3}$
$V_{flow} = 1000 \text{ km s}^{-1}$	

addition of  $C_2$  units and the inclusion of pentagon rings in large PACs. However, new experiments suggest that fullerene molecules are formed in a H-free gas from the coalescence of large monocyclic rings in the gas phase (Rubin et al. 1991; von Helden et al. 1993; Kroto 1994) and rule out the role of PACs as intermediates.

As for the formation of AC grains, the reactivity of large carbon clusters was studied by Zhang and co-workers (1986) who showed that odd-numbered, spherical clusters from the fullerene family could not form a perfectly closed, unreactive shell and were highly reactive due to their dangling, unsatisfied valences. This was observed in the final depletion of injected radicals and odd-number fullerenes in the experiment. It was further suggested that these odd-number clusters were reacting with small clusters present in large amount in the gas to form large icospiral AC structures and grains.

Therefore, we would expect chains, large rings, fullerenes and AC particles to form in the winds of cool WC stars. Aromatic molecules are characterized by several vibrational stretching modes from their carbon skeleton (Allamandola et al. 1989) searched for aromatic emission bands at 6.2 and 7.7  $\mu\text{m}$  in several WC stars with the ISO SWS06 instrument. No obvious strong emission features were observed supporting the view that PACs may not represent a large carbon cluster population in the winds.

Silicon carbide is a common condensate in the outflows of carbon-rich, AGB stars. In a gas rich in hydrogen, solid SiC is produced in the laboratory from various techniques, in particular the combined IR pyrolysis of hydrocarbon molecules and silane ( $\text{SiH}_4$ ). Although the nucleation mechanisms still need to be identified, it is observed that Si,  $C_2$  and  $\text{SiC}_2$  molecules are among the gas phase intermediates in the condensation zone where SiC clusters form (Fantoni et al. 1991). The synthesis of SiC clusters in the laboratory usually involves the breakdown of small hydrocarbons and their reaction with atomic Si. In a gas poor in hydrogen, the nucleation reactions are certainly very different, but the intermediate species should be similar because they represent the only compounds which can be formed in a mixture of atomic silicon and carbon.

### 3. The model

In this paper, we restrict our study to the formation of precursors to dust grains, that is, small linear clusters up to  $C_6$ . We also investigate the formation of silicon-bearing species, with special attention to potential intermediates in the formation of silicon

**Table 2.** Elemental composition (in mass fraction) of the stellar surface (from Prantzos et al. 1986, 1987) and ionization fraction in the wind (from van der Hucht et al. 1986).

Elemental Composition	Ionization fraction
A(He)= 0.6	[HeII]/[HeI] = 0.9 : 0.1
A(C)= 0.4	[CIII]/[CII] = 0.5 : 0.5
A(O)= 0.23	[CI]/[CII] = 0
A(Si)= 0.1	[OII]/[OI] = 1 : 0
A(S)= 0.03	[SiII]/[SiI] = 1 : 0 = [SII]/[SI]

carbide clusters. Below, we discuss the stellar model and the various chemical processes considered.

#### 3.1. Stellar parameters

We consider for our model a ‘typical’, single WC9 star whose parameters are listed in Table 1. The values are chosen to represent a class of stars which are persistent dust makers but we do not try to reproduce any star in particular.

The value for the effective temperature was chosen in accord with the stellar radiation fields and ionization ratios modelled by van der Hucht et al. (1986, hereafter HCW). We also list the parameters characterising the inner dust shells from the models of WHT. The local gas number density at the inner radius is derived from the assumption of constant mass loss and that the stellar wind has been fully accelerated before the dust forming region. More recent non-LTE modelling of the WC9 star WR104 by Crowther (1997) gives a higher effective temperature ( $T_{eff} \sim 45000 \text{ K}$ ) and a smaller stellar radius ( $R_{\star} = 3R_{\odot}$ ). The luminosity, and therefore the inner edge of the dust shell (in physical units) and the wind density there would be comparable to those in Table 1 if WC104 was a single star heating the dust.

The chemical abundances in the wind listed in Table 2 are from the evolutionary models of Prantzos et al. (1986, 1987) and are comparable to the composition of WR104 determined by Crowther (1997). The ionization fraction is that calculated by HCW for the emission line forming region at  $\sim 2 R_{\star}$ . They calculated that the ionization fraction should decrease by less than 10% when reaching the radio photosphere but we ignore this small drop and adopt the values of the line forming region at large radii.

#### 3.2. The chemical model

The chemistry involves 390 reactions listed in Appendix A and 53 chemical species listed in Table 3. We consider all types of reactions possibly taking place in a plasma bathed in a strong radiation field, i.e., neutral-neutral reactions, ion-molecule processes, electronic and radiative recombinations, radiative association reactions, associative detachment reactions, and photoprocesses. The reaction rates were taken from the UMIST data base (Millar et al. 1997) or derived from other sources. In particular, care was given to the temperature dependence of certain classes of reactions as the chemical rates are usually mea-

**Table 3.** Chemical species considered to be present or to form in the wind of a WC9 star.

He	He <sup>+</sup>	C	C <sup>+</sup>	C <sup>2+</sup>	C <sup>-</sup>	O	O <sup>+</sup>
O <sup>-</sup>	Si	Si <sup>+</sup>	S	S <sup>+</sup>	S <sup>-</sup>	C <sub>2</sub>	C <sub>2</sub> <sup>+</sup>
C <sub>2</sub> <sup>-</sup>	C <sub>3</sub>	C <sub>3</sub> <sup>+</sup>	C <sub>3</sub> <sup>-</sup>	C <sub>4</sub>	C <sub>4</sub> <sup>+</sup>	C <sub>4</sub> <sup>-</sup>	C <sub>5</sub>
C <sub>5</sub> <sup>+</sup>	C <sub>5</sub> <sup>-</sup>	C <sub>6</sub>	C <sub>6</sub> <sup>+</sup>	C <sub>6</sub> <sup>-</sup>	CO	CO <sup>+</sup>	CO <sub>2</sub>
CO <sub>2</sub> <sup>+</sup>	O <sub>2</sub>	O <sub>2</sub> <sup>+</sup>	CS	CS <sup>+</sup>	S <sub>2</sub>	S <sub>2</sub> <sup>+</sup>	SO
SO <sup>+</sup>	SO <sub>2</sub>	SO <sub>2</sub> <sup>+</sup>	OCS	OCS <sup>+</sup>	SiO	SiO <sup>+</sup>	SiS
SiS <sup>+</sup>	SiC	SiC <sup>+</sup>	SiC <sub>2</sub>	SiC <sub>2</sub> <sup>+</sup>			

sured or calculated for low temperatures. For example, at the high temperatures considered in our study, we have assigned an inverse temperature dependence to the associative detachment processes involving the small carbon clusters, following Moruzzi et al. (1968). We have ignored at this stage of the model the dissociation and ionisation of species induced by cosmic rays. We also assume that there is no penetration of the UV interstellar radiation field at the inner edge of the dust shell and just consider the stellar radiation field as the dominant source of all photo-processes.

We include bimolecular and termolecular processes and consider that the chemical reactions proceed both in the forward and backward directions. This is especially important for the case of a high density wind. When no backward rate is documented, we estimate the rate from thermodynamical data as described by Cherchneff et al. (1992) and Willacy & Cherchneff (1998). This results in a backward rate

$$k_b = AT^n C^{\Delta\nu} \exp \left\{ \frac{\Delta G_R - E_\alpha}{RT} \right\} \quad (1)$$

where  $A$ ,  $n$  and  $E_\alpha$  are the Arrhenius parameters for the forward reaction,  $C = N \times 10^6 / RT$  is the conversion factor from atmosphere to  $\text{cm}^{-3}$  units,  $\nu$  the stoichiometric factor of the forward reaction,  $N$  is the Avogadro number,  $R$  the perfect gas constant, and  $T$  the gas temperature.  $\Delta G_R$  is the Gibbs free energy for the forward reaction at 1 atmosphere of total gas pressure and is calculated from the Gibbs free energies of formation,  $\Delta G_f$ , of the reactants and products. These data were taken from the JANAF thermochemical data tables (Chase et al. 1985). For  $\text{SiC}_2$ , we used data derived by Willacy & Cherchneff (1998).

Silicon and sulphur are present in the wind of WC stars and their abundances are not solar reflecting helium-core burning nucleosynthesis. As the star is also carbon-rich, one would expect silicon carbide to form in the wind as it forms in carbon-rich AGB objects. However, the  $11.3 \mu\text{m}$  emission band is not seen in the near-IR spectral distribution of the star. In order to check if chemistry is partially responsible for the lack of SiC, we investigate the formation of gas-phase, silicon- and sulphur-bearing species which are potential intermediates in the nucleation and condensation of silicon carbide clusters, and consider the same types of reactions as for the carbon-oxygen gas. Many rates are not documented for the reactions involving Si and S and we use the isovalence of silicon with carbon, and sulphur with oxygen to derive unknown chemical rates from documented data. This approach has been used by Willacy & Cherchneff (1998) for

**Table 4.** References for documented photo-process cross-sections.

Processes		Reference
He	→ He <sup>+</sup> + e <sup>-</sup>	Band et al. 1990
C	→ C <sup>+</sup> + e <sup>-</sup>	Cantù et al. 1981 Hofmann et al. 1983
C <sup>+</sup>	→ C <sup>++</sup> + e <sup>-</sup>	Henry 1970
C <sub>2</sub>	→ C + C	Pouilly et al. 1983
C <sub>2</sub>	→ C <sub>2</sub> <sup>+</sup> + e <sup>-</sup>	Padial et al. 1985
CO	→ C + O	Letzelter et al. 1987
CO	→ CO <sup>+</sup> + e <sup>-</sup>	Hudson 1971
CO <sub>2</sub>	→ CO + O	Hitchcock et al. 1980
CO <sub>2</sub>	→ CO <sub>2</sub> <sup>+</sup> + e <sup>-</sup>	Hudson 1971 Hitchcock et al. 1980
CO <sub>2</sub>	→ CO <sup>+</sup> + O + e <sup>-</sup>	Hitchcock et al. 1980
CO <sub>2</sub>	→ CO + O <sup>+</sup> + e <sup>-</sup>	Hitchcock et al. 1980
CO <sub>2</sub>	→ C <sup>+</sup> + O <sub>2</sub> + e <sup>-</sup>	Hitchcock et al. 1980
O	→ O <sup>+</sup> + e <sup>-</sup>	Taylor & Burke 1976
O <sub>2</sub>	→ O + O	Brion & Tan 1979
O <sub>2</sub>	→ O <sub>2</sub> <sup>+</sup> + e <sup>-</sup>	Brion & Tan 1979 Ogawa & Ogawa 1975 Clark & Wayne 1970
O <sub>2</sub>	→ O + O <sup>+</sup> + e <sup>-</sup>	Brion & Tan 1979

modelling the chemistry of silicon and sulphur-bearing species in the carbon-rich AGB star IRC+10216 and results in good agreements between theoretical and observational molecular abundances.

### 3.3. Photo-processes

The processes induced by absorption of radiation are photo-dissociation, photo-ionisation and photo-fragmentation. We calculated the rates for each type of photo-processes based on experimental cross-sections when available and have used the radiation field calculated by HCW at the pseudo-photosphere of a WC star with effective temperature  $T_{eff} = 19000$  K. The stellar spectrum differs greatly from that of a 19000 K blackbody because of the various edges due to ionisation of helium and carbon. The first ionisation of carbon C I at  $1100 \text{ \AA}$  provides the dominant UV opacity in the wind and results in a drop of almost two orders of magnitude in the radiation flux. Therefore, the C I edge enhances the chance of survival of most molecular species against dissociation by UV radiation.

The stellar radiation field was fitted by several polynomials of degree 4 as a function of wavelength from the far-UV to the visible parts of the spectrum. References for the documented cross-sections are listed in Table 4.

The cross-section data and the stellar radiation field were subdivided in various wavelength bands and the rates for each band were then calculated assuming a constant cross-section over the band. The total rate is obtained as the sum of all the rate contributions from all the spectral bands and is given by

$$k_{photo} = W \int_0^{+\infty} \sigma_\lambda F(\lambda) \frac{\lambda}{hc} d\lambda \quad (2)$$

**Table 5.** Dominant formation (top line) and destruction (bottom line) processes in the chemical model. **Formation** – RA: radiative association; AD:  $e^-$  associative detachment; RXXX: reaction No. XXX in Appendix A; CE: charge exchange - **Destruction** – PP: photo-processes (dissociation, ionisation); R: recombination;  $He^+$ :  $He^+$  attack;  $C^+$ :  $C^+$  attack; O: O attack; RXXX: reaction No. XXX in Appendix A

Gas number density	$C_2$	$C_n$	CO	$O_2$	CS	SiO	SiC	SO	Chain Ions
$10^6 - 10^8$ $cm^{-3}$	RA PP, $He^+$	RA PP, $He^+$	RA PP, $He^+$	RA PP, $He^+$	RA PP	RA, CE PP, $He^+$	RA PP, $He^+$	RA PP	RA PP, R
$10^9 - 10^{10}$ $cm^{-3}$	RA $He^+$	RA, AD $He^+$ , PP	RA, AD $He^+$	RA $He^+$ , $C^+$	RA, AD, CE $He^+$ , PP	R281 $C^+$ , $He^+$	AD $C^+$ , $He^+$	R305, AD PP, $He^+$ , $C^+$	RA R
$10^{11} - 10^{13}$ $cm^{-3}$	RA, AD O, $He^+$	RA, AD O, $He^+$	RA, AD $He^+$	RA, AD $C^+$	CE, R304 O, $He^+$	R281 O, $He^+$	AD $C^+$	R305 $C^+$	RA, CE R

$$= W \sum_{i=1}^n \sigma_i F_i(\lambda) \frac{\lambda}{hc} \Delta_i \lambda, \quad (3)$$

where  $\sigma_i$  is the constant cross-section over band  $i$ ,  $F_i(\lambda)$  is the fit to the radiation field over band  $i$ ,  $\Delta_i \lambda$  is the width for band  $i$  and  $W = \frac{1}{4} (R/r)^2$  is the dilution factor at large distances from the star. The resulting rates are very large compared with the usual rates encountered in circumstellar or interstellar models because of the very strong radiation field and the fact that we have ignored wind opacity at UV wavelengths (see Appendix A).

Photo-fragmentation of molecular species is usually important at energies of  $\sim 10$  eV, i.e., for photons in the far-UV part of the stellar spectrum and cross-sections have been measured for many species. It involves the breaking in various ionic fragments following photo-ionisation of the neutral species in excited states. However, as the stellar radiation field drops sharply at wavelengths smaller than 1100 Å, fragmentation is never among the dominant photo-processes.

For a few molecules there are no available data on cross-sections and we make use of the photo-rates from the UMIST database (Millar et al. 1997) estimated for the interstellar radiation field of Draine (1978). We then rescale the value to the WC stellar radiation field, assuming a constant cross-section over the entire wavelength range. This method was tested on a few molecules for which experimental cross-sections were known, and gave rates which were off by at most a factor five from the initial values. Such discrepancy has no dramatic effect on the calculation as photo-processes are the dominant destruction channels in our model only for low gas number densities (see Sect. 4).

We expect carbon monoxide to self-shield against photo-dissociation by UV photons if formed but have not included a treatment of CO self-shielding in the present calculations. Our results on CO abundances can then be considered as lower limits.

## 4. Results

A system of coupled, stiff, first-order differential equations describing the chemistry has been solved between the inner radius of the dust shell  $R_{inner}$  and  $R_{inner} + 5 R_*$ , assuming the constant gas temperature of Table 1 and the wind chemical composition of Table 2. We assume that no molecules are initially present at

the inner radius of the dust shell. In order to test the chemistry we vary the conditions at  $R_{inner}$  and study the effect on the nucleation of dust precursors. We consider gas number densities at the inner radius ranging from  $10^6$  to  $10^{13}$   $cm^{-3}$ , allow the gas temperature to vary from 1000 to 6000 K and introduce an arbitrary wind opacity in the UV ( $\lambda \leq 1100$  Å) for a gas number density of  $10^{10}$   $cm^{-3}$ .

The results after integration between  $R_{inner}$  and  $R_{inner} + 5 R_*$  and for various gas number densities at  $R_{inner}$  are shown in Figs. 2–4. A constant gas temperature of 4000K and no wind opacity are assumed. It is clear from inspection of these figures that the chemistry is highly dependent on the gas number density. At the low density given by the spherically symmetric wind model (see Table 1), the dominant species in the gas are atomic ions while as the gas number density increases, the recombination of ions takes place and the gas composition is governed by neutral-phase chemistry, that is, the dominant species are neutral atoms and molecules although electrons and some ions are still present in relatively large amounts (for example,  $C^+$ ,  $O^+$  and  $He^+$ ).

We can identify three density regimes over which the dominant formation and destruction processes vary: the low density range ( $n_{gas} = 10^6 - 10^8$   $cm^{-3}$ ), the intermediate density window ( $n_{gas} = 10^9 - 10^{10}$   $cm^{-3}$ ), and finally the high density range ( $n_{gas} = 10^{11} - 10^{13}$   $cm^{-3}$ ). The processes at play for these three density windows are summarized in Table 5 and we discuss in turn results on carbon and silicon species below.

### 4.1. Carbon-bearing species

As illustrated in Fig. 3, small carbon chains are extremely sensitive to the gas density as all the chain abundances vary by  $\sim 20$  orders of magnitude over the density range considered. This variation is due to the shift in the chemistry as the gas density increases from ionic to neutral, and the changes in formation and destruction processes shown in Table 5.

At low gas densities, the dominant formation processes for  $C_2$ , the carbon chains and the dominant C-bearing molecular species (CO, CS) are radiative association (RA) reactions, such as



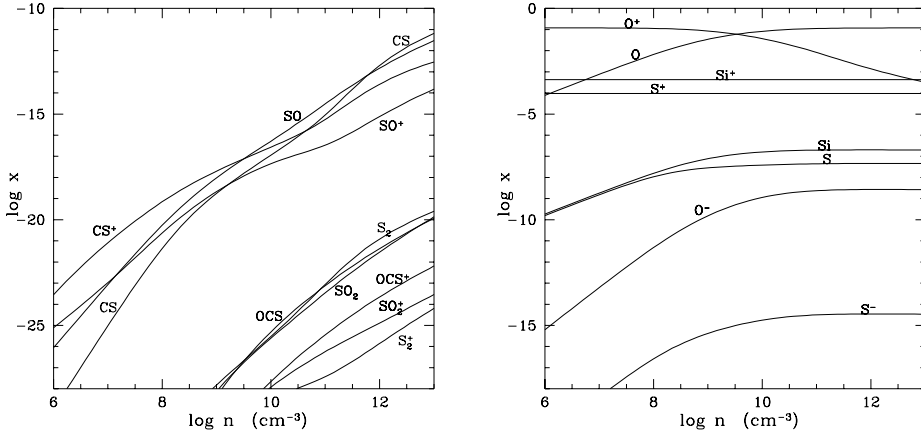


**Fig. 2.** Abundances of atoms and their ions as a function of gas number density at the inner dust shell radius. The gas temperature is that of Table 1.

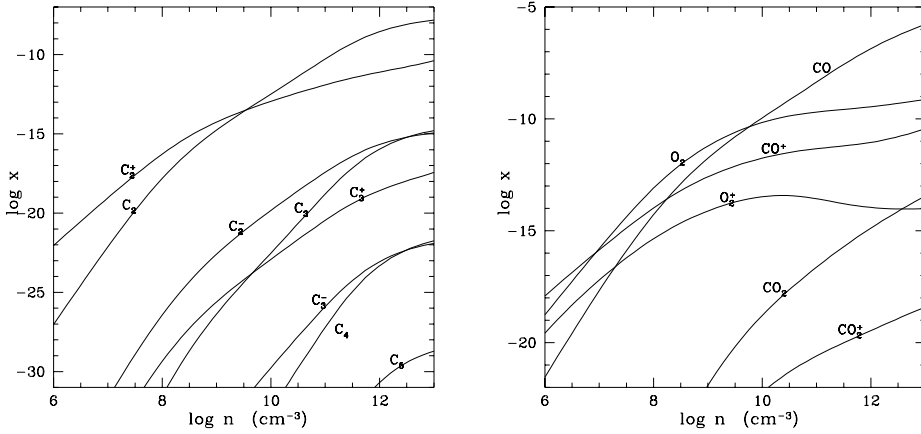


**Fig. 3.** Molecular abundances as a function of gas number density at the inner dust shell radius (The gas temperature is that of Table 1) – Left: carbon chains – Right: C and O-bearing species.

Destruction of the chains, CO and CS results from photo-processes (dissociation and ionisation) at low densities while  $\text{He}^+$  attack as



starts to play a role as the density increases.

In the intermediate density range, a new type of formation channel appears, that is, associative detachment (AD) reactions such as



where  $\text{C}^-$  is formed from radiative recombination reactions. However, radiative association reactions still represent the dominant formation mechanism for the chains and the dominant carbon-bearing species. Destruction is now essentially governed by  $\text{He}^+$  attack and  $\text{C}^+$  attack such as



while photo-processes become less important.

For still larger densities, formation occurs mainly via radiative association reactions and to a less extent, associative detachment processes. As for the destruction of molecules, a new destructive channel becomes dominant and involves the attack by atomic oxygen, i.e.,



while  $\text{He}^+$  and  $\text{C}^+$  attacks become less important. This result illustrates the shift in the chemistry as the gas density increases and the fact that ions recombine more efficiently at higher densities. Once the neutral gas phase dominates, the destruction processes for molecules and their ions arise from atomic oxygen attack. Because we have ignored CO self-shielding in the treatment of our photo-processes, more atomic oxygen not locked up in CO is available in the flow, leading to more effective destruction of carbon chains.

Apart from  $\text{C}_2$ , the final abundances of small carbon clusters and their ions are never large even at high gas number densities, due to the fact that the formation processes involved are slow radiative association and associative detachment reactions. Carbon monoxide is the dominant molecular species to form at high densities, but unlike late-type, carbon stars, it does not lock up the entire oxygen in this carbon-rich environment. The wind is still rich in free He, C and O atoms and their ions, and the observational evidence for the absence of other types of dust, such as oxides, is puzzling. We shall discuss this point in Sect. 5.

#### 4.2. Silicon and sulphur species

Several silicon and sulphur-bearing species are considered, in particular molecules involved in the process of SiC cluster con-

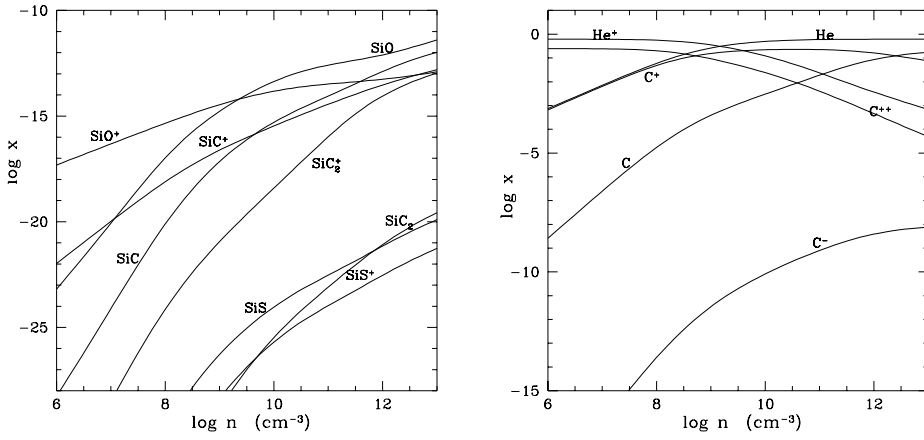


**Fig. 4.** Molecular abundances as a function of gas number density at the inner dust shell radius (The gas temperature is that of Table 1) – Left: Silicon species – Right: Sulphur species.

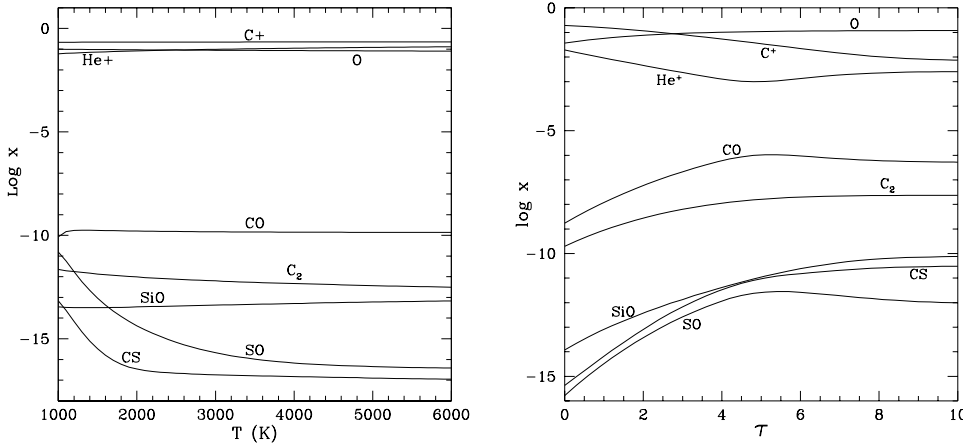


**Fig. 5.** Left: Molecular abundances as a function of gas temperature at the inner dust shell radius. The gas number density is  $10^{10} \text{ cm}^{-3}$  and  $\tau_{UV} = 0$ . Right: Molecular abundances as a function of gas optical depth at the inner dust shell radius.  $T = 4000 \text{ K}$ ,  $n(\text{gas}) = 10^{10} \text{ cm}^{-3}$ .

densation. The formation and destruction processes for silicon and sulphur species are summarised in Table 5 and are similar to those involved in the formation of carbon species, except for a few specific reactions at play in the formation of CS, SiO or SO. Results on chemical abundances are presented in Fig. 4 and indicate that the dominant species are CS, SiO, SO and SiC and that the trend displayed by carbon-bearing molecules, that is, increasing abundances with increasing gas number densities, is also followed by these molecules. However, the final abundances are quite low at large densities, especially for the species which could act as intermediates in the nucleation of silicon carbide (e.g.,  $\text{SiC}_2$ ,  $\text{SiC}_2^+$ ). As previously mentioned, SiC has not been observed at  $11.3 \mu\text{m}$  in the wind of WC stars, but this can be understood in the light of the present results. Again, the difficulty in building SiC dust molecular precursors may reside in the slow chemical reactions governing the formation mechanism.

#### 4.3. Temperature and opacity variations

Variation of the gas temperature at the inner dust shell was also considered for the various density regimes to check if the chemistry was very sensitive to temperature. Results are presented in Fig. 5 for the intermediate density range and the dominant

chemical species in the wind. Apart from  $\text{C}_2$ , CS and SO, the atomic and molecular abundances do not show much variation with temperature. This is mainly due to the fact that the destruction and formation processes for these species are similar at low and high gas temperatures and that their chemical rates do not depend strongly on temperature. The situation is different for  $\text{C}_2$ , CS and SO which show higher abundances at low temperatures. For  $\text{C}_2$ , the destruction processes remain the same over the temperature range considered, but an extra formation channel (associative detachment) adds up to radiative association reactions at low temperatures and increases the total net formation rate. For CS and SO, the formation processes are very different at high and low temperatures. At high temperatures, RA reactions dominate while neutral-neutral reactions are more important at low T. As the latter channels are usually characterized by faster chemical rates than RA processes, this results in a greater net formation rate at low temperatures. These results hold at lower and higher gas densities than  $10^{10} \text{ cm}^{-3}$  and imply that the chemistry of dust precursors is quite temperature independent.

Results induced by considering an arbitrary wind opacity in the UV are also presented in Fig. 5. All molecular species show increasing abundances with increasing wind opacity and this is understood quite simply by the fact that the  $\text{He}^+$  abun-

dance drops of two orders of magnitude as the opacity becomes larger. In the intermediate density region, the main destruction processes are  $\text{He}^+$  and  $\text{C}^+$  attacks (see Table 5) and photo-processes, and a higher wind opacity results in less ionisation of helium and carbon and lower photo-rates. Therefore, molecular destruction is hindered by the opacity of the wind.

## 5. Discussion

Previous studies of dust formation in WC stars (Zubko 1998) have considered the growth of grains via collisions of charged particles with carbon ions but did not tackle the nucleation of grains from the gas phase. As winds of Wolf-Rayet stars are far from equilibrium, the investigation of dust formation requires a non-equilibrium approach using a specific chemical reaction scheme. The present study based on a chemical kinetic description shows that dust precursors and molecular species form in significant amounts for high gas density *only*. There has long been observational evidence for inhomogeneities in the wind of WR stars. Clumps have been proposed to explain the transient narrow emission features appearing in the optical emission spectra of these stars (Moffat et al. 1988; Brown et al. 1995). Furthermore, theoretical models aiming at explaining the radiative acceleration of the wind above the stellar surface predict the formation of strong shocks which would trigger the formation of high density regions in the acceleration zone (Owocki et al. 1988). These clumps would then be momentum-coupled to the wind and travel with the terminal outflow velocity. Brown et al. proposed an average gas density enhancement in the clumps of a few hundreds compared to the homogeneous wind in the line forming region, that is, a region much closer to the star than the inner dust shell radius considered in the present study. The eclipse phenomena observed by Veen et al. (1998) and Crowther (1997) occur also quite close to the stellar surface and prove that dust formation in WC9 stars does occur in clumps. Notwithstanding the fact that the location of these observed clumps imply harsher conditions for grain formation than those considered in this study, we consider that clumps in WC9 stellar winds can play a significant role in the formation of their dust shells.

Another source of density enhancement which might help molecule formation and dust condensation is the “wind-compressed zone” (WCZ), resulting from the transfer of matter to the equatorial plane from high latitude regions due to the star’s rotation and wind (Cassinelli 1995; Ignace et al. 1996). The equatorial to “uniform wind” density contrast depends on the relative rotational and wind velocities and is of the order of a few. However the higher opacity in the WCZ allows dust formation to occur closer to the star, raising the density advantage to about an order of magnitude over the uniform wind case, and spectropolarimetry provides evidence for such flattened winds around some WR stars (Schulte-Ladbeck et al. 1991).

Finally, one type of structure in the stellar wind which could provide the density enhancements required for dust formation is the compressed material formed in colliding wind binaries. Compression of the wind by a factor of  $\sim 10^3$  can occur within the shock if the wind cools sufficiently by radiation (Usov 1991).

Most of episodic dust makers appear to be members of binary systems (Williams 1998) and one of them, the WC7 + O4-5 system WR140, has had an orbit determined. The orbit is very eccentric and this star makes dust for a few months only during each periastron passage. Since the WR and O star winds in WR140 collide and compress wind material all the time, the episodic dust formation is attributed to the greater pre-shock density ( $\sim 100$  times that during most of the orbit) at this phase, when the wind-collision region has moved closer to the WC7 star (Williams 1998).

The chemistry describing the formation of small carbon linear clusters appears to be quite independent of temperature, which implies that molecules could form closer to the star as long as they are shielded from the stellar radiation field. A closer location would also result in higher gas densities and perhaps lower ionisation fraction if high opacities are provided either by clumps or WCZs.

Under the wind conditions considered in this study, our chemical scheme cannot account for the formation of large amounts of carbon clusters.  $\text{C}_2$  is the only carbon chain which forms quite efficiently at high densities, while the abundance of  $\text{C}_6$  remains always very low. The chemical model is robust enough because we have included all possible reaction channels at play in a hydrogen-deficient gas. However, it is important to bear in mind that many of the chemical reaction rates used in the chemical scheme have been theoretically predicted or measured for the low gas temperatures encountered in the laboratory or the interstellar medium. High temperatures may generate higher chemical rates and rate predictions at elevated temperatures are therefore badly needed. It is also possible that metals such as iron or aluminum could act as catalysts in the building-up of carbon clusters as it is known to happen with hydrocarbons and aromatic molecules (Chaudret et al. 1991) and this point should be investigated in more details.

If carbon clusters are difficult to nucleate, the situation for silicon carbide looks even more drastic. Although the formation of  $\text{SiC}_2$  and  $\text{SiC}_2^+$  species increases at larger gas density, wind opacity and lower gas temperature, it seems difficult to form large amounts of silicon bearing species. Again, this is mainly due to the fact that the formation processes for these molecules are the slow radiative association and associative detachment reactions. The situation is quite different in the wind of carbon-rich, AGB stars where AC and SiC solids are observed to form on a continuous basis and are responsible for the large mass loss rates of these objects. The inner wind where the dust forms is hydrogen-rich and characterised by high gas densities and cooler temperatures than in WC winds. A wealth of hydrogen-bearing molecules, in particular acetylene ( $\text{C}_2\text{H}_2$ ), is already present in the stellar photosphere at thermal equilibrium and due to the ubiquity of hydrogen in the wind, hydrocarbon radicals form and react with other neutral species. These neutral-neutral reactions are characterised by much higher reaction rates than those of the processes active in WC stars and trigger the efficient nucleation of carbon dust (Cherchneff et al. 1992).

Another surprising fact is the non-detection of other possible condensates in WC wind. If higher gas densities are considered

(for example, the intermediate density regime), inspection of Fig. 2 shows that there is still a large amount of atomic oxygen in the outflow. Furthermore, certain elements like silicon, magnesium and aluminum are present in the stellar wind with relatively large abundances. Therefore, some solid oxides as  $\text{SiO}_x$  or  $\text{MgO}_x$ , alumina ( $\text{Al}_2\text{O}_3$ ) and silicates, which typically form in oxygen-rich AGB stars, could theoretically form because of the wind chemical composition. However, the difficulty in forming oxygen-bearing dust may be again a consequence of the lack of hydrogen. In AGB winds for example, the formation of dust precursor molecules such as  $\text{SiO}$  or  $\text{SiO}_2$  involves reactions with atomic silicon and the hydroxyl radical, OH.

We conclude that dust formation in single WC9 stars must take place under physical conditions very different from the “very favourable” wind parameters considered in this study as the chemistry leading to grain nucleation and condensation can *only* occur via slow chemical processes. Indeed, with new evidence for higher effective temperatures and stronger radiation fields characterising late WC stars, it seems that very large densities and opacities are required for molecule and dust formation. These densities and opacities could be found in the clumps forming close to the stellar surface and future studies on dust in WC9 stars will include a chemical kinetic treatment of dust formation in clumps close to the stellar surface with treatment of the ionisation fraction, temperature and opacity for inhomogeneities bathed in a strong radiation field. Finally, the prediction that large amounts of carbon monoxide form in these hydrogen-poor, high density regions is not too surprising as CO has been detected in other hydrogen-poor environments such as the ejecta of type II supernova (Meikle et al. 1989). Therefore, the present results call for the observational detection of carbon monoxide in the winds of late, carbon-rich Wolf-Rayet stars.

*Acknowledgements.* The authors are grateful to E. Herbst for very helpful comments on some of the chemical processes, to P. D. Singh for help with rates for radiative association reactions, and to R. Ignace for useful comments on wind-compressed-zones.

## References

- Allamandola L.J., Tielens A.G.G.M., Barker J.R., 1989, ApJS 71, 733  
 Allen D.A., Harvey P.M., Swings J.P., 1972, A&A 20, 333  
 Band I.M., Trzhaskovskaya M.B., Verner D.A., Yakovlev D.G., 1990, A&A 237, 267  
 Baulch D.L., Cobos C.J., Cox R.A., et al., 1994, J. Phys. Chem. Ref. Data 23, 847  
 Brion C.E., Tan K.H., 1979, J. El. Spect. Rel. Phen. 17, 101  
 Brown J.C., Richardson L.L., Antokhin I., et al., 1995, A&A 295, 725  
 Cantù A.M., Mazzoni M., Pettini M., Tozzi G.P., 1981, Phys. Review A 23, 1223  
 Cassinelli J.P., 1995, In: van der Hucht K., Williams P.M. (eds.) Wolf Rayet Stars: Binaries, Colliding Winds, Evolution. IAU Symposium 163, Kluwer, Dordrecht, p. 191  
 Chase M.W., Davies C.A., Downey J.R., et al., 1985, J. Phys. Chem. Ref. Data 14, Suppl. 1, 1  
 Chaudret B., Le Beuze A., Rabaa H., Saillard J.Y., Serra G., 1991, New J. Chem. 15, 791  
 Cherchneff I., 1997, Ap&SS 251, 333  
 Cherchneff I., Tielens A.G.G.M., 1995, In: van der Hucht K., Williams P.M. (eds.) Wolf Rayet Stars: Binaries, Colliding Winds, Evolution. IAU Symposium 163, Kluwer, Dordrecht, p. 346  
 Cherchneff I., Barker J.R., Tielens A.G.G.M., 1992, ApJ 401, 269  
 Clark I.D., Wayne R.P., 1970, Mol. Phys. 18, 523  
 Crowther P.A., 1997, MNRAS 290, L59  
 Draine B.T., 1978, ApJS 36, 595  
 Dyck H.M., Simon T., Wolstencroft R.D., 1984, ApJ 277, 675  
 Fantoni R., Bijnen F., Djurić N., Piccirillo S., 1991, Appl. Phys. B 52, 176  
 Heath J.R., 1992, In: Hammond G.S., Kuck V.J. (eds.) Fullerenes. ACS Symposium 481, ACS, p. 1  
 Henry R.J.W., 1970, ApJ 161, 1153  
 von Helden G., Gotts N.G., Bowers M.T., 1993, Nat 363, 60  
 von Helden G., Gotts N.G., Palke W.E., Bowers M.T., 1994, Int. J. Mass Spect. and Ion Proc. 138, 33  
 Hitchcock A.P., Brion C.E., van der Wiel M.J., 1980, Chem. Phys. 45, 461  
 Hofmann H., Saha H.P., Trefftz E., 1983, A&A 126, 415  
 Hudson R.D., 1971, Review of Geophysics & Space Physics 9, 305  
 Ignace R., Cassinelli J.P., Bjorkman J.E., 1996, ApJ 459, 671  
 Kroto H.W., Heath J.R., O'Brien S.C., Curl R.F., Smalley R.E., 1985, Nat 318, 162  
 Kroto H.W., 1994, Int. J. Mass Spect. and Ion Proc. 138, 1  
 Letzelter C., Eidelsberg M., Rostas F., 1987, Chem. Phys. 114, 273  
 Meikle W.P.S., Allen A.A., Spyromilio J., Varani G.-F., 1989, MNRAS 238, 193  
 Millar T.J., Farquhar P.R.A., Willacy K., 1997, A&AS 121, 139  
 Moffat A.F.J., Drissen L., Lamontagne R., Robert C., 1988, ApJ 334, 1038  
 Moruzzi J.L., Ekin J.W., Phelps A.V., 1968, J. Chem. Phys. 48, 3070  
 Ogawa S., Ogawa M., 1975, Canadian J. Phys. 53, 1845  
 Owocki S.P., Castor J.I., Rybicki G.B., 1988, ApJ 335, 914  
 Padial N.T., Collins L.A., Schneider B.I., 1985, ApJ 298, 369  
 Pouilly B., Robbe J.M., Schamps J., Roueff E., 1983, J. Phys. B 16, 437  
 Prantzos N., Doom C., Arnould M., de Loore C., 1986, ApJ 304, 695  
 Prantzos N., Arnould M., Arcoragi J.P., 1987, ApJ 315, 209  
 Rubin Y., Kahr M., Knobler C.B., Diederich F., Wilkins C.L., 1991, J. Am. Chem. Soc. 113, 495  
 Schulte-Ladbeck R.E., Nordsieck K.H., Taylor M., et al. 1991, ApJ 382, 301  
 Shemilov K.B., Hunter J.M., Jarrold M.F., 1994, Int. J. Mass Spect. and Ion Proc. 138, 17  
 Taylor K.T., Burke P.G., 1976, J. Phys. B 9, L353  
 Usov V.V., 1991, MNRAS 252, 49  
 van der Hucht K.A., 1997, Ap&SS 251, 311  
 van der Hucht K., Cassinelli J.P., Williams P.M., 1986, A&A 168, 111  
 van der Hucht K., Williams P.M., Morris P.W., 1996, A&A 315, L193  
 Veen P., van Genderen A.M., van der Hucht K.A., et al., 1998, A&A 329, 199  
 Willacy K., Cherchneff I., 1998, A&A 330, 676  
 Williams P.M., 1997, Ap&SS 251, 321  
 Williams P.M., van der Hucht K., Thé P.S., 1987, A&A 182, 91  
 Williams P.M., van der Hucht K., Morris P.W., 1997, In: Waters R., Waelkens C., van der Hucht K. (eds.) ISO's view on Stellar Evolution. Kluwer, Dordrecht, in press  
 Zhang Q.L., O'Brien S.C., Heath J.R., et al., 1986, J. Phys. Chem 90, 525  
 Zubko V.G., 1998, MNRAS 295, 109